

Effects of Near-Fault Ground Shaking on Sliding Systems

G. Gazetas, M.ASCE¹; E. Garini²; I. Anastasopoulos³; and T. Georgarakos⁴

Abstract: A numerical study is presented for a rigid block supported through a frictional contact surface on a horizontal or an inclined plane, and subjected to horizontal or slope-parallel excitation. The latter is described with idealized pulses and near-fault seismic records strongly influenced by forward-directivity or fling-step effects (from Northridge, Kobe, Kocaeli, Chi-Chi, Aegion). In addition to the well known dependence of the resulting block slippage on variables such as the peak base velocity, the peak base acceleration, and the critical acceleration ratio, our study has consistently and repeatedly revealed a profound sensitivity of both maximum and residual slippage: (1) on the sequence and even the details of the pulses contained in the excitation and (2) on the direction (+ or -) in which the shaking of the inclined plane is imposed. By contrast, the slippage is not affected to any measurable degree by even the strongest vertical components of the accelerograms. Moreover, the slippage from a specific record may often be poorly correlated with its Arias intensity. These findings may contradict some of the prevailing beliefs that emanate from statistical correlation studies. The upper-bound sliding displacements from near-fault excitations may substantially exceed the values obtained from some of the currently available design charts.

DOI: 10.1061/(ASCE)GT.1943-5606.0000174

CE Database subject headings: Sliding; Seismic effects; Ground motion; Symmetry; Asymmetry.

Introduction

Ground shaking in the close neighborhood of a rupturing seismic fault may be affected by wave propagation effects known as “forward directivity” and by tectonic deformations producing a permanent ground offset known as “fling step.” The former effect is the outcome of the coherent arrival of seismic waves emitted from a seismogenic fault when its rupturing propagates toward the site. It manifests itself with a single long-period high-amplitude pulse occurring near the beginning of shaking, and oriented perpendicularly to the fault (Somerville 2000). The fling-step effect is the outcome of the tectonic permanent deformation of the earth in the proximity of the fault. It manifests itself in the record with a static residual displacement, oriented parallel to the fault strike with strike-slip earthquakes and perpendicular to the fault with purely dip-slip (normal or thrust) earthquakes (Abrahamson 2001).

Fig. 1(a) is a sketch, of a strike-slip event, portraying the idealized “signatures” of the two phenomena on the *fault-normal* and *fault-parallel* components of the displacement record. Fig. 1(b) depicts two remarkable accelerograms, TCU-068 (from Chi-Chi 1999) and Fukiai (from Kobe 1995) exhibiting fling-step and forward-directivity effects, respectively. The velocity time history

of TCU-068 contains a large pulse (2.6 m/s) of huge duration (6.3 s), which is consistent with the permanent ground offset of about 8 m that can be seen in the derived displacement record, and which has actually been observed in the field. The derived velocity time history of Fukiai contains several cycles with a devastating maximum velocity step $\Delta V \approx 2.3$ m/s. The destructive capacity of this quantity was first elaborated by Bertero et al. (1976).

A significant amount of research has been devoted to the two phenomena, especially in the aftermath of the Northridge, Kobe, Kocaeli, and Chi-Chi earthquakes. That research has so far focused: first, on identifying, interpreting, and mathematically representing the effects of “directivity” and “fling” on the ground motions (Singh 1985; Somerville 2000,2003; Abrahamson 2001; Makris and Roussos 2000; Mavroeidis and Papageorgiou 2003; Hisada and Bielak 2003; Bray and Rodriguez-Marek 2004; Haward et al. 2005); then, on developing empirical predictive relationships for the parameter characterization of the directivity or fling related pulses (Somerville et al. 1997; Bray and Rodriguez-Marek 2004; Xie et al. 2005); and finally, on assessing the potential of directivity and fling pulses to inflict damage in a variety of geotechnical and structural systems (for example, Bertero et al. 1978; Singh 1985; Hall et al. 1995; Gazetas 1996; Kramer and Smith 1997; Iwan et al. 2000; Sasani and Bertero 2000; Makris and Roussos 2000; Alavi and Krawinkler 2000; Jangid and Kelly 2001; Pavlou and Constantinou 2004; Shen et al. 2004; Mavroeidis et al. 2004; Xu et al. 2006; Changhai et al. 2007).

The work presented here belongs in the latter category. It summarizes studies on the effects of near-fault motions on two idealized sliding systems: (1) a rigid block in contact with (resting on) a horizontal base; (2) a rigid block resting on an inclined plane, of angle β (Fig. 2). In both cases the contact between structure and base is rigid-ideally plastic, obeying Coulomb’s friction law with a constant coefficient of friction, μ . The horizontal or inclined base is subjected to parallel excitation, i.e., horizontal motion in Case 1 and motion inclined at an angle β in Case 2. Furthermore, the effect of a simultaneous vertical acceleration

¹Professor, Laboratory of Soil Mechanics, National Technical Univ., Athens 15342, Greece (corresponding author).

²Ph.D. Student, Laboratory of Soil Mechanics, National Technical Univ., Athens 15342, Greece.

³Adjunct Lecturer, Laboratory of Soil Mechanics, National Technical Univ., Athens 15342, Greece.

⁴Ph.D. Student, Laboratory of Soil Mechanics, National Technical Univ., Athens 15342, Greece.

Note. This manuscript was submitted on September 22, 2008; approved on June 10, 2009; published online on November 13, 2009. Discussion period open until May 1, 2010; separate discussions must be submitted for individual papers. This paper is part of the *Journal of Geotechnical and Geoenvironmental Engineering*, Vol. 135, No. 12, December 1, 2009. ©ASCE, ISSN 1090-0241/2009/12-1906–1921/\$25.00.

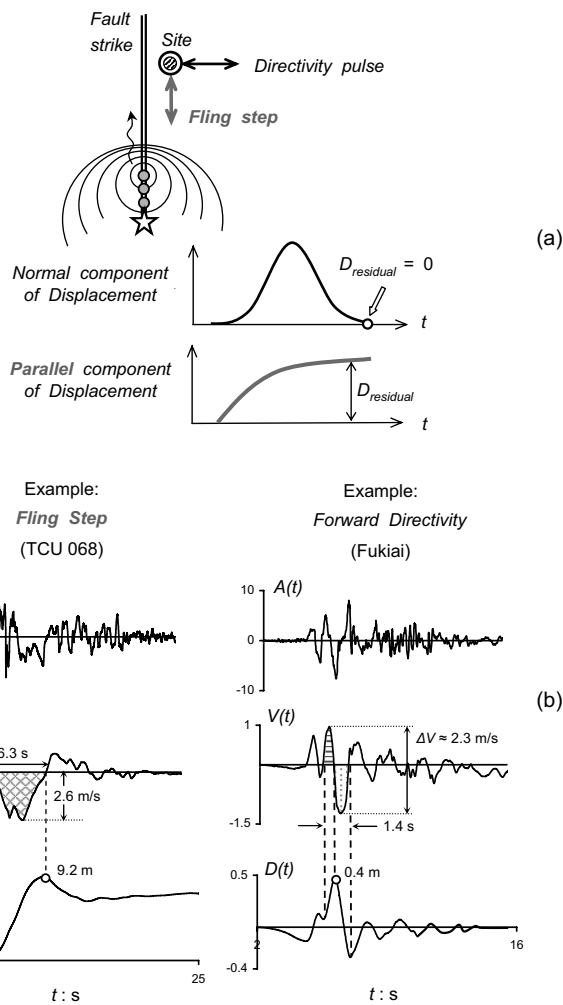


Fig. 1. (a) Schematic explanation of the forward-directivity and fling-step phenomena as reflected in the displacement records; (b) examples of actual accelerograms bearing the “signature” of the two effects: TCU-068 record (Chi-Chi 1999) and Fukiai record (Kobe 1995)

time history is also explored for Case 1, while a horizontal and a vertical acceleration are also imposed in Case 2. As excitation we utilize idealized wavelets and near-fault seismic records strongly influenced by forward-directivity or fling-step effects (Northridge 1994; Kobe 1995; Kocaeli 1999; Chi-Chi 1999; Aegion 1995). Some additional records are also used for comparison.

The destructive potential of long duration acceleration pulses, which is one of the outcomes of directivity and fling effects, has been demonstrated in the pioneering work of Bertero et al. (1976) in connection with the heavy damage of the Olive View Hospital during the San Fernando 1971 earthquake. One of the significant conclusions of his research was that:

“The types of excitation that induce the maximum response in elastic and non-elastic systems are fundamentally different and hence one can not derive the maximum non-elastic response from the corresponding elastic one” (Bertero et al. 1976).

The preceding remark has motivated our choice of the ideally rigid-plastic constant-friction systems: in addition to their obvious direct use in earthquake engineering, they are representative of extremely inelastic behavior. The anticipation was that such sys-

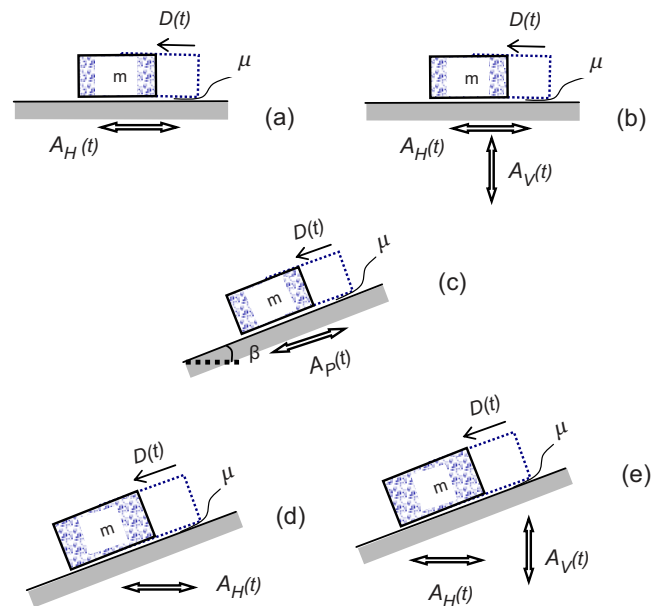


Fig. 2. Five rigid block problems studied in the paper: [(a) and (b)] sliding on horizontal plane undergoing only-horizontal and horizontal-and-vertical motion, respectively; (c) sliding on inclined plane excited by motion parallel to the slope; [(d) and (e)] sliding on inclined plane undergoing only-horizontal and horizontal-and-vertical motion, respectively

tems would be far more sensitive than the purely linear elastic systems (the other extreme of reality) to the peculiarity of near-fault ground shaking. The results presented in the paper confirm this expectation.

Further objectives of our research are:

- To quantify the maximum and permanent slippage as a function: (1) of the amplitude and duration of the near-fault pulses; (2) of the nature of the main pulse and the number and sequence of pulses.
- To discuss the differences between symmetric and asymmetric sliding (Cases 1 and 2), and to explore the importance of the direction (+ or -) of a particular near-fault excitation in the asymmetric Case 2.
- To investigate the role of large vertical accelerations simultaneously acting with horizontal accelerations, as is appropriate for near-fault motions.

It is hoped that a deeper insight will be gained from our study into the nature and consequence of directivity- and fling-affected motion. However, the development of design charts/equations to complement the presently available statistical relations is only a secondary goal of this paper.

Seismic Sliding of Rigid Block on Horizontal Plane

This problem is of direct application to seismic base isolation of rigid structures using low-friction bearings, and to isolation of embankments from the underlying ground using geosynthetic liners. Moreover, in an indirect qualitative sense, it can be considered as an analog for a host of geotechnical and earthquake problems, such as the response of a stiff soil crust on an underlying soft thin layer, the sliding of a stiff light structure with surface foundation on dense ground, the in-ground isolation of

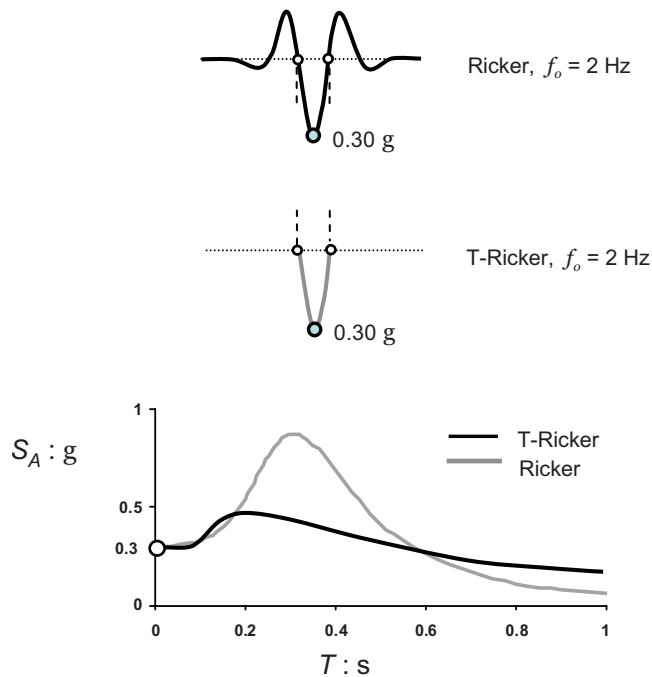


Fig. 3. Two idealized time histories (“wavelets”) used as base excitation, with their response acceleration spectra $S_A: g-T$ (peak ground acceleration: 0.30g)

structures using geomembranes. Perhaps equally important is the resemblance of the restoring force-displacement mechanism of this system to that of a very stiff elastoplastic system.

The mechanics of the system are well understood and need no further explanation here. The rigid block, simply resting on a base with an interface obeying Coulomb’s friction law with a single coefficient of friction μ , will experience accelerations that cannot exceed, by Newton’s law, a critical value

$$A_C \equiv \alpha_C g = \mu g \quad (1)$$

As long as the peak ground acceleration $A_H \equiv \alpha_H g$ does not exceed A_C in absolute value, the block does not slide but moves with the ground. When $A_H \equiv \alpha_H g$ surpasses $A_C = \mu g$ the block acceleration remains constant (and equal to μg), and sliding takes place until the velocities of the block and the ground equalize. At that moment, if ground acceleration is smaller than the critical acceleration, $A_C = \mu g$, sliding stops.

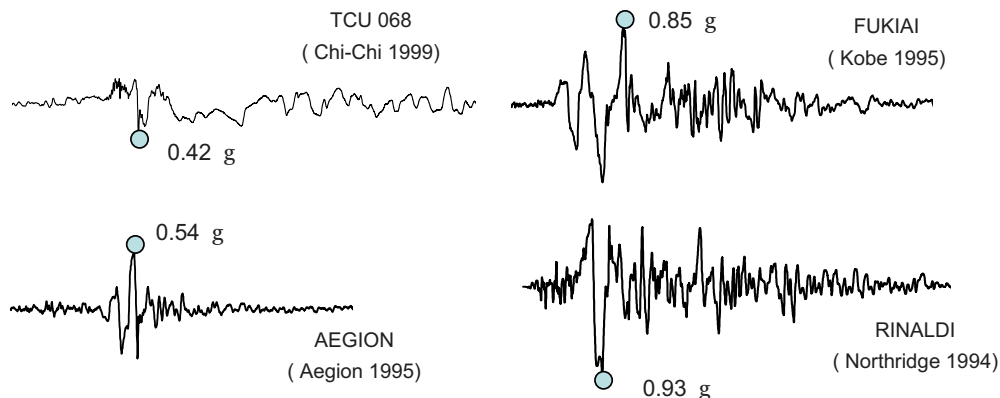


Fig. 4. Accelerograms of actual near-fault recordings used in the paper (all time histories are in the same time and amplitude scale)

The penalty for limiting the block acceleration to the level of the coefficient of friction is a sliding displacement (“slippage”), which is found to be dependent on four basic variables:

- The maximum peak ground acceleration $A_H \equiv \alpha_H g$.
- The dominant frequency f_0 of ground excitation.
- The ratio μ/α_H .
- The form and the details of the ground excitation.

A large number of analyses were performed to understand the influence of these variables. Only the highlights are presented in the sequel.

Excitation

Two idealized wavelets are used as simple representation of near-fault pulses (Fig. 3):

- A three-pulse Ricker “wavelet,” described by its amplitude $A_H = \alpha_H g$ and characteristic frequency f_0 .
- A one-pulse truncated Ricker wavelet (“T-Ricker”) which is derived from the original wavelet by ignoring the first and last half-cycles.

Moreover, we also use three well-known actual accelerograms from the near-fault worldwide bank of records: Rinaldi (Northridge 1994), Fukiai (Kobe 1995), TCU-068 (Chi-Chi 1999), and Aegion (Aegion 1995). Fig. 4 shows these records.

Dimensional Analysis and Characteristic Results

It is easily shown that the maximum sliding displacement, D , can be expressed in one of the following alternative nondimensional expressions

$$\frac{Df_0^2}{A_H}$$

or

$$\frac{DA_H}{V_H^2} = F_{\text{unc}} \left(\frac{\mu}{a_H}; \text{shape and sequence of pulse(s)} \right) \quad (2)$$

Note that the dimensionless variables on the left-hand side of Eq. (2) had already been suggested in the seminal work of Newmark 1965. The preceding dimensionless expression is quite similar with the one presented by Yegian et al. (1991a) [see also Kramer (1996)].

The great importance of the dominant (“characteristic”) frequency of excitation, f_0 , is obvious: for given acceleration ampli-

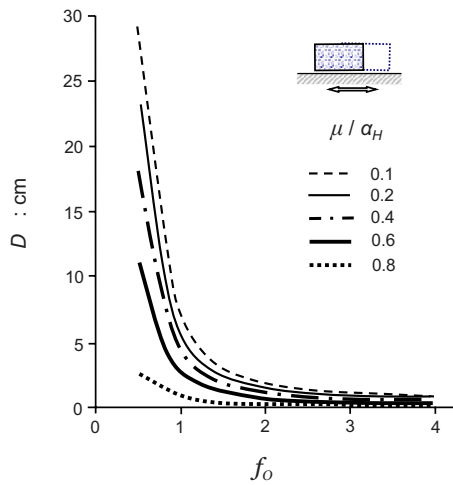


Fig. 5. Effect of characteristic frequency, f_0 , and of μ/α_H ratio on maximum slippage (excitation: single pulse of T-Ricker wavelet)

tude A_H and nature of pulses, D is inversely proportional to f_0^2 . Fig. 5 portrays this dependence for a T-Ricker type excitation with $A_H=0.60g$.

Influence of μ/α_H Ratio: Safe Gulf Paradox

In view of Eq. (2), the expectation of course would be that F_{unc} is a monotonically decreasing function of μ/α_H —the latter ratio playing the role of an instantaneous factor of safety against sliding. In other words, one might have expected a monotonic decrease of slippage with increasing friction coefficient μ for a given excitation. The results prove that this is not always the case. Fig. 6 displays (parametrically with respect to f_0) the dimensionless maximum slippage in terms of the μ/α_H ratio for a Ricker excitation. It reveals that, while initially the slippage increases with the reduction of μ/α_H , it reaches a peak value for $\mu/\alpha_H \approx 0.4$, beyond which it decreases until the value $\mu/\alpha_H \approx 0.2$, where a local minimum is observed before its final ascent with further decreasing μ/α_H . Apparently, an unexpected safe gulf exists, which would be beneficial in design—a value of μ smaller than about $0.40\alpha_H$ can be chosen (e.g., $\mu=0.20\alpha_H$) with which

both structural acceleration *and* slippage are reduced below their $\mu=0.40\alpha_H$ values. This phenomenon is caused by the presence of the first (preceding) smaller cycle in the Ricker wavelet which, as the friction coefficient decreases, causes increasingly more substantial slippage in the opposite direction (Fig. 7). For the (truncated) T-Ricker excitation, where these two cycles are absent, no such a safe gulf is observed, and slippage increases monotonically with decreasing μ (Fig. 8). Evidently, the wavelet *form* and details are of crucial importance—at least as much as the *dominant frequency* and the *intensity* of the motion.

Excitation with Near-Fault Accelerograms: Further Surprising Results

To verify and further reinforce the validity of the aforementioned conclusions, analyses with real records have been performed. A few characteristic results are highlighted here.

First, to develop a deeper insight into the similarity between the Ricker wavelet and actual directivity-affected motions, Fig. 9(a) compares the Rinaldi record (Northridge, 1994) to a fitted Ricker wavelet ($A_H \approx 0.90g$, $f_0 \approx 1$ Hz). Despite the complexity of real motions, the resulting sliding behavior of a block excited by the two motions is qualitatively similar, as seen in Fig. 9(b). But, surprisingly at first glance, the Ricker motion is twice as detrimental as the actual motion, despite the significantly larger duration of the latter. The culprit of this unexpected behavior is something deceptively small: the larger (not smaller) acceleration amplitudes of Rinaldi between a and b (i.e., between about 0.16–2.10 s)! This stronger excitation, coming 0.20 s before the main damaging pulse (of $A_H \approx 0.90g$), “displaces” the block significantly in the opposite direction and thus reduces its final slippage—another evidence of the important role of the (quite unpredictable) detailed sequence of pulses. Note that the Arias Intensity of the Ricker “wavelet” is only 3.2 compared to 7.1 of the record.

A second example is given in Fig. 10. The directivity-affected Aegion accelerogram (recorded in the $M=6.4$ earthquake of 1995) is characterized by a peak acceleration $A_H=0.54g$ at a dominant period of about 0.60 s (Gazetas 1996). A block supported through a coefficient of friction $\mu=0.054$ (i.e., α_C/α_H

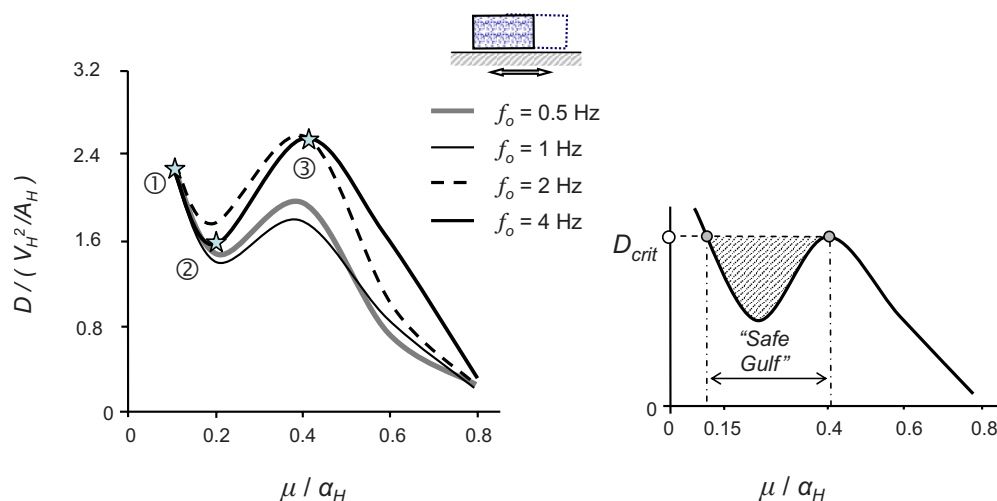


Fig. 6. Effect of μ/α_H ratio on the dimensionless maximum sliding, for different Ricker characteristic frequencies, f_0 . Observe the “paradoxical” reduction of D , with decreasing μ/α_H , for $\mu/\alpha_H < 0.4$, which leads to an additional safe gulf for lower values of the μ/α_H ratio.

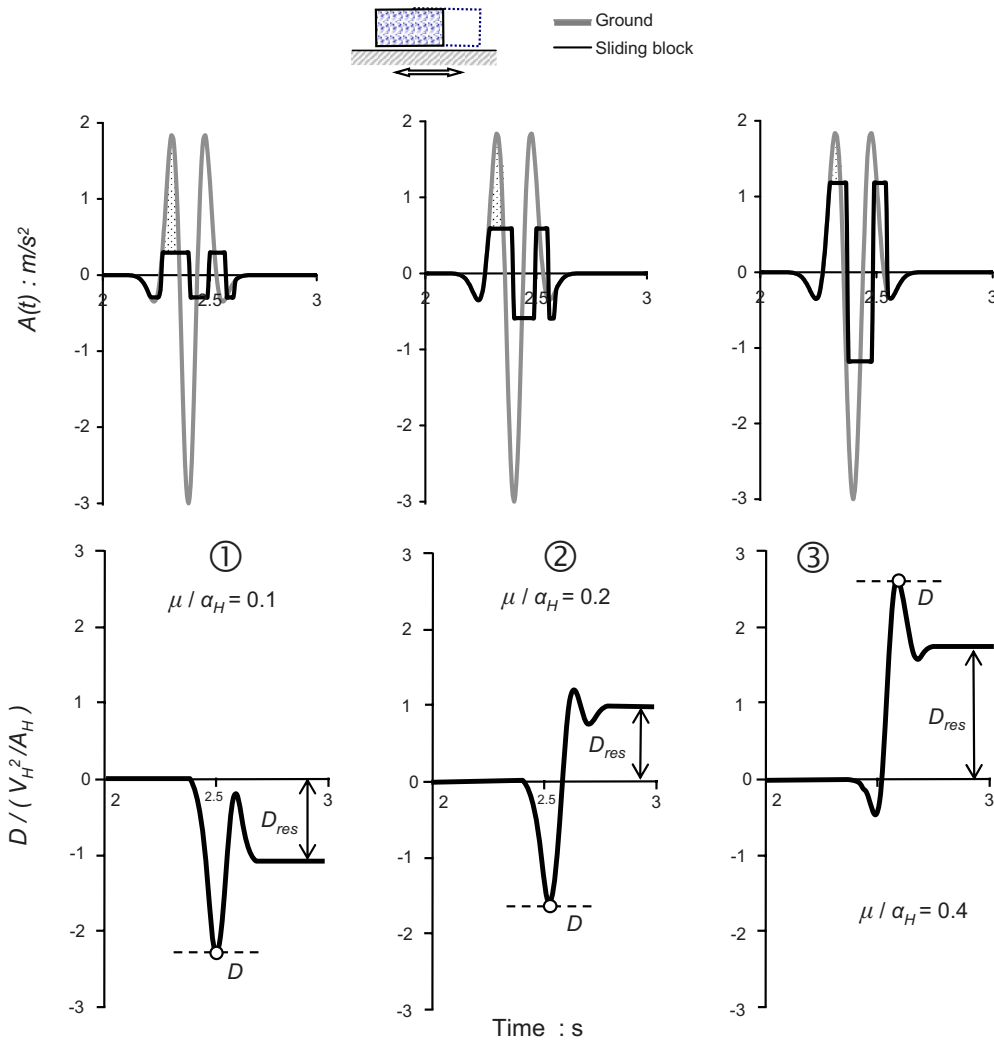


Fig. 7. Explanation of the safe gulf paradox of Fig. 6: acceleration and sliding-displacement time histories for a single wavelet frequency $f_o = 4$ Hz and different values of μ / α_H ratio (0.1, 0.2, and 0.4)

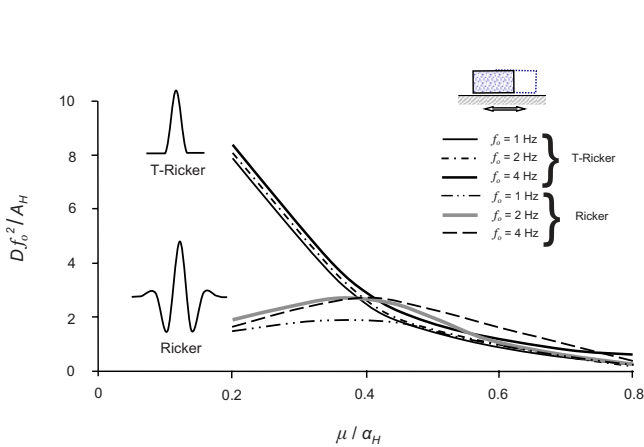


Fig. 8. Dimensionless maximum sliding for Ricker and T-Ricker excitation, for different values of the wavelet frequency but same amplitude A_H . Notice the dramatic effect of the type of excitation.

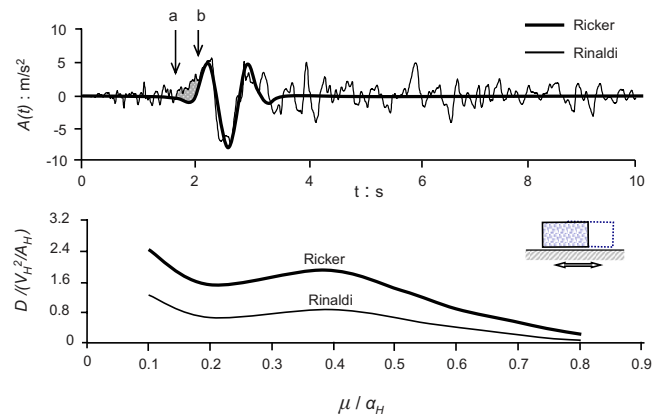


Fig. 9. Approximation of the Rinaldi-228^o record with a simple Ricker wavelet (top plot). Comparison of sliding induced by these two motions (bottom plot). Despite the similarity in the form of the resulting curves the (smaller duration) Ricker excitation leads to two times higher displacements.

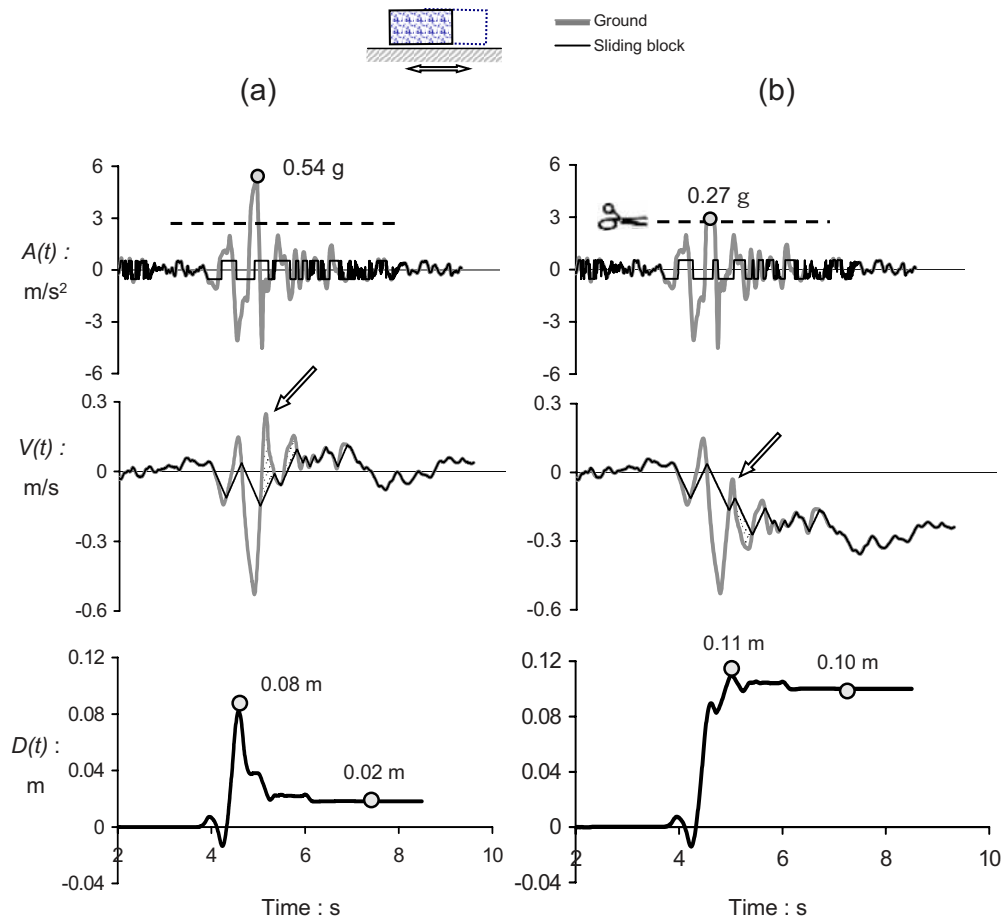


Fig. 10. Paradoxical effect of “trimming” the peak ground acceleration of the Aegion record is illustrated in terms of acceleration, velocity, and slippage time histories for a block on a horizontal plane with $\alpha_C/\alpha_H=0.1$. The beneficial role in this particular case of the 0.54g peak, in breaking and reversing the sliding, is undermining by its removal.

=0.1) experiences the acceleration, velocity, and sliding-displacement histories shown in Fig. 10(a). When the large acceleration pulse is cut off at its middle, the slippage of the block paradoxically increases. The provided velocity time histories of the ground and the block in Fig. 10(b) help resolve the paradox. For this particular excitation and this specific ratio of α_C/α_H , the role of the 0.54g pulse is beneficial: it “puts the breaks” and reverses the sliding—hence the maximum slippage is $D=0.08$ m and the residual merely $D_{res}=0.02$ m. The trimming of this pulse to half of its original peak value undermines somewhat the “breaking” action and eliminates most of the “reversing” action—hence $D=0.11$ m and $D_{res}=0.10$ m!

A *third* example: comparison of the sliding potential of the two components of the Chi-Chi TCU-068 record. Significant fling effects are present in these components which are portrayed in Fig. 11(a), with their response spectra compared in Fig. 11(b).

Notice that the east-west (EW) component has greater peak acceleration compared to the north-south (NS) component (0.50g to 0.36g); in addition, its spectral acceleration values are also higher over broad period ranges. Hence, one might have anticipated the largest slippage to occur with the EW component. Reality [Fig. 11(c)] shows quite the opposite by a large margin (2.5 to 1 for the peak slippage, and 5 to 1 for the residual)! This is clearly due exclusively to the long-duration one-sided pulse that is contained in the NS record.

The reader should not fail to notice that in all the aforementioned three examples the *largest slippage* was each and every

time associated with one or more of the following:

- With the *smaller* peak ground acceleration.
- With the *smaller* Arias intensity.
- With the *smaller* strong motion duration.
- Not even with the *larger* response spectrum (except in few cases).

One should therefore be cautious when using empirical statistical correlations (which anticipate the opposite trend) to predict the response in *individual* cases. This of course does not necessarily negate the role of statistical correlations in probabilistic seismic risk analyses.

Simultaneous Horizontal and Vertical Accelerations: Dispelling a Persevering Myth

Earthquake engineers have always been concerned about the effects of the vertical component of ground acceleration. In recent years the issue of the possible effects of vertical acceleration on different structural sliding systems such as seismically isolated bridges and buildings has been debated. Large vertical accelerations recorded in numerous earthquakes have fueled the discussion in the subject. Geotechnical engineers appear to have accepted the important role of vertical acceleration for retaining structures and slopes. The vectorial synthesis of α_H and α_V appears as a natural fact in many papers and textbooks on the subject. But is α_V really significant for sliding systems?

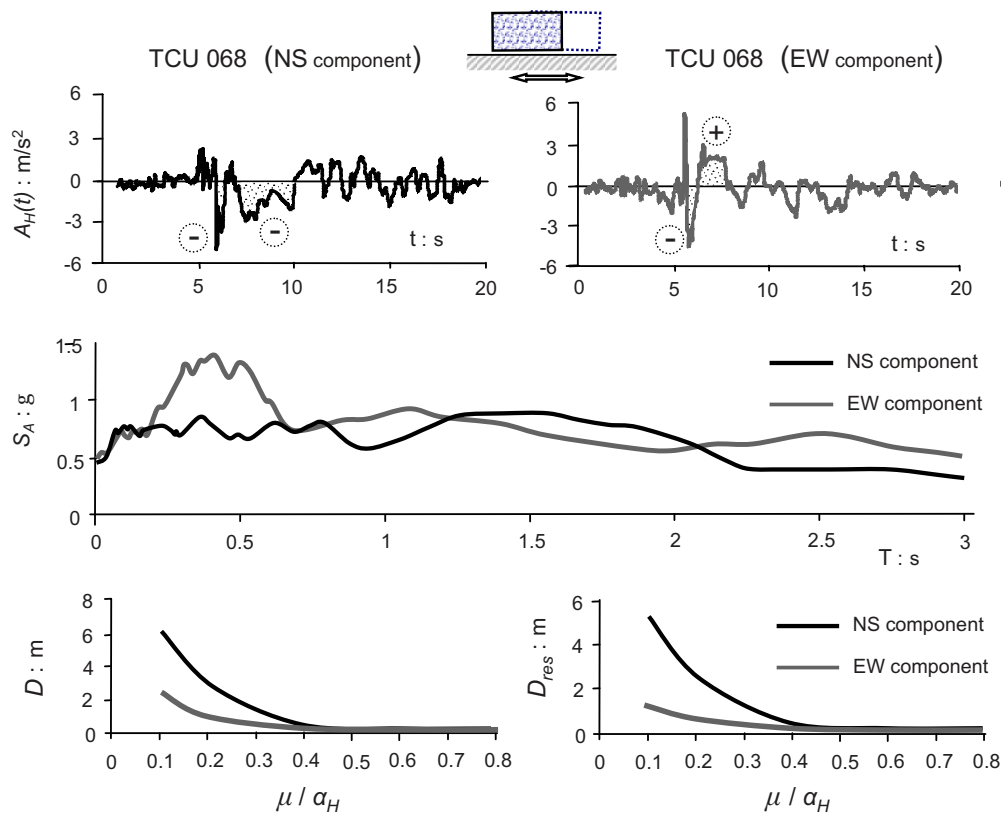


Fig. 11. Example of the importance of “details” of excitation on sliding. Although the EW component of the TCU-068 record (gray color) has a larger peak acceleration and larger spectral accelerations for a wide range of periods, the sliding displacements produced by the NS component (black color) are higher by a factor of almost 3.

To explore the subject, a comprehensive parameter study has been conducted using both *idealized* and *actual* horizontal and vertical acceleration time histories. Only a summary of the results is highlighted next.

In actual records, the vertical component of the ground acceleration is of a much higher frequency content than its horizontal components—a fact arising from the nature of the *P* and *S* waves which dominate the vertical and horizontal ground motion, respectively. Exceptions to this rule are not rare. Hence, to be more general in our investigation with idealized motions, a broad range of dominant periods of vertical motion (up to $T_V \approx 0.50$ s) has been studied.

We begin with results using actual motions: pairs of horizontal and vertical components of accelerograms recorded within a few kilometers from the fault (where the vertical component is usually at its strongest). Only two characteristic results are shown here, for:

- Rinaldi (Northridge): $A_H \approx 0.94g$, $A_V \approx 0.85g$ (forward directivity affected).
- TCU-068 (Chi-Chi): $A_H \approx 0.42g$, $A_V \approx 0.50g$ (fling step affected).

The two components of the two records are plotted for comparison in Fig. 12. The resulting curves of the maximum slippage, D , versus μ/α_H are portrayed in Fig. 13. Two curves are compared in each plot: one for excitation by the horizontal component alone, and the other for the simultaneous excitation by the horizontal and vertical components (Fig. 13). Apparently, even the occurrence of very strong vertical accelerations is of no significance for the slippage of rigid blocks! A second conclusion from Fig. 13 is that for this *symmetric* sliding problem, the fling-

affected Chi-Chi record, with its huge velocity pulse (as will be shown in Fig. 15 in the sequel), is far more detrimental than the directivity-affected Northridge record.

It is interesting to focus on the Chi-Chi record, the vertical acceleration of which seems to be particularly severe, containing a strong and exceptionally long-period pulse (0.3g, 2.5 s) which leads to uncommonly high (for vertical motion) spectral acceleration values (Fig. 12). Yet the analysis proves that the effect of such a vertical excitation would cause a mere 4% increase of the maximum and residual values of slippage (see Fig. 14).

Numerous additional results with the Ricker wavelets as horizontal and vertical excitation have completely verified the aforementioned conclusions. Space limitations do not allow the presentation of these results. But the reader should not be surprised that even when the two components are identical and their peak values coincide in time (a very severe and rather unlikely incident), the vertical excitation still has a minor effect [see Fardis et al. (2003), Garini and Gazetas (2007)]. In fact it could not be determined a priori whether this effect would be *positive* or *negative*. Therefore, neglecting it altogether will have no measurable consequence.

Seismic Sliding of Rigid Block on Inclined Plane

In earthquake geotechnical engineering the analog of dynamic sliding of a block on an inclined plane has been in use for estimating the response of earth dams, embankments, and retaining walls during earthquakes. Introduced in 1965 by Newmark, the

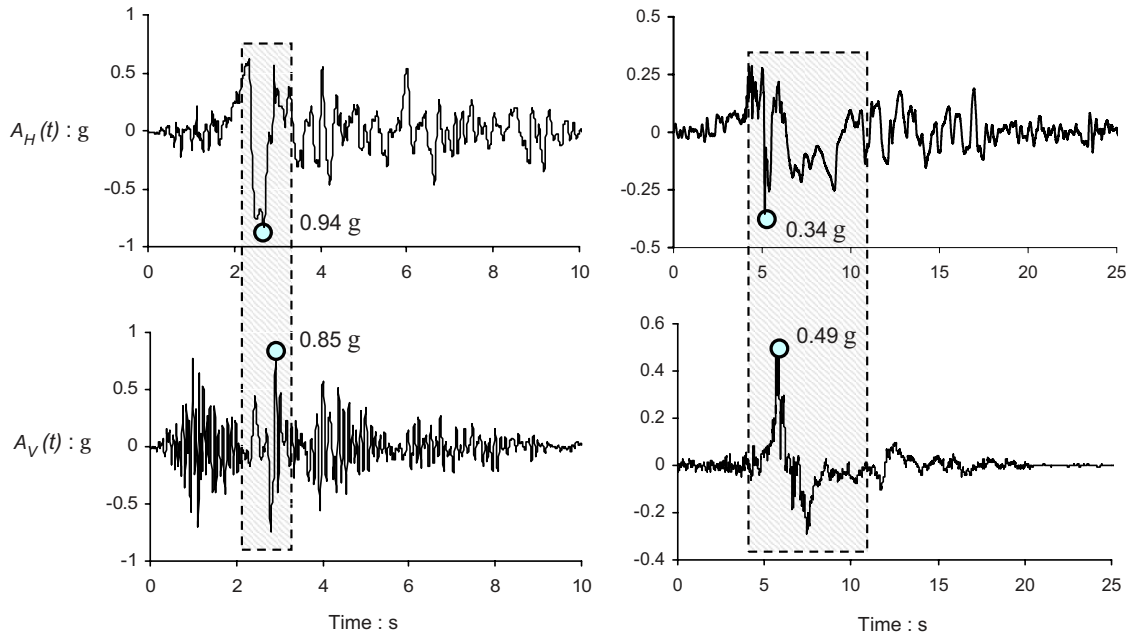


Fig. 12. Rinaldi and TCU-068 horizontal and vertical records of the 1994 Northridge and 1999 Chi-Chi earthquakes. The near-fault effects appear at almost the same time in both components, horizontal, and vertical. Notice the very high vertical accelerations.

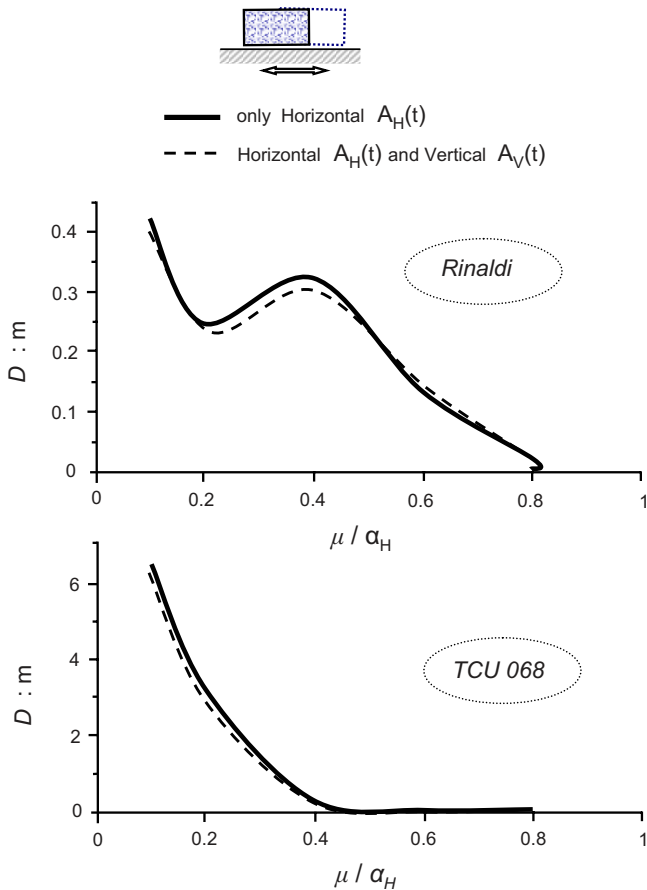


Fig. 13. Maximum sliding displacements for actual accelerograms with and without the simultaneous effect of their vertical component. Vertical excitation has an insignificant effect.

analog was further used by Seed and Martin (1966), Ambraseys and Sarma (1967), and Makdisi and Seed (1978) who developed procedures for predicting the permanent displacements of dams, while Richards and Elms (1979) adopted it for evaluating the response of gravity retaining walls and later of shallow foundations. Also, numerous other researchers, including Sarma (1975), Franklin and Chang (1977), Gazetas et al. (1981), Lin and Whitman (1983), Constantinou et al. (1984), Constantinou and Gazetas (1987), Ambraseys and Srbulov (1995), Yegian et al. (1998,1991a,b), Gazetas and Uddin (1994), Gazetas (1996), Kramer and Smith (1997), Rathje and Bray (2000), Travararou (2003), Bray and Travararou (2007), and Kramer and Lindwall (2004), have used and extended Newmark's model in analyzing various aspects of the problem, in deterministic or probabilistic terms. Laboratory shaking table experiments, such as those by Yegian and Lahlaf (1992), Fishman et al. (1995), and Wartman et al. (2003) have demonstrated the usefulness of sliding block analysis for the estimation of earthquake triggered plastic deformations. Other applications of the "sliding block on inclined plane" concept include the dynamic analyses of landfills with geosynthetic liners by Yegian et al. (1998) and by Bray and Rathje (1998), Rathje and Bray (2000); and the seismic response of concrete gravity dams "allowed" to slide, by Fenves and Chopra (1986), Leger and Katsouli (1989), and Danay and Adeghe (1993).

For the block of Fig. 1(c), the largest value of acceleration that can develop depends on the direction of shaking. When an acceleration pulse acts from left to right ("upward"), the inertial force on the block acts downhill and cannot exceed the critical value

$$\alpha_{C1} = \mu \cos \beta - \sin \beta \quad (3)$$

Whereas in the opposite direction ("downward" base motion) the inertia acts uphill and cannot exceed

$$\alpha_{C2} = \mu \cos \beta + \sin \beta \quad (4)$$

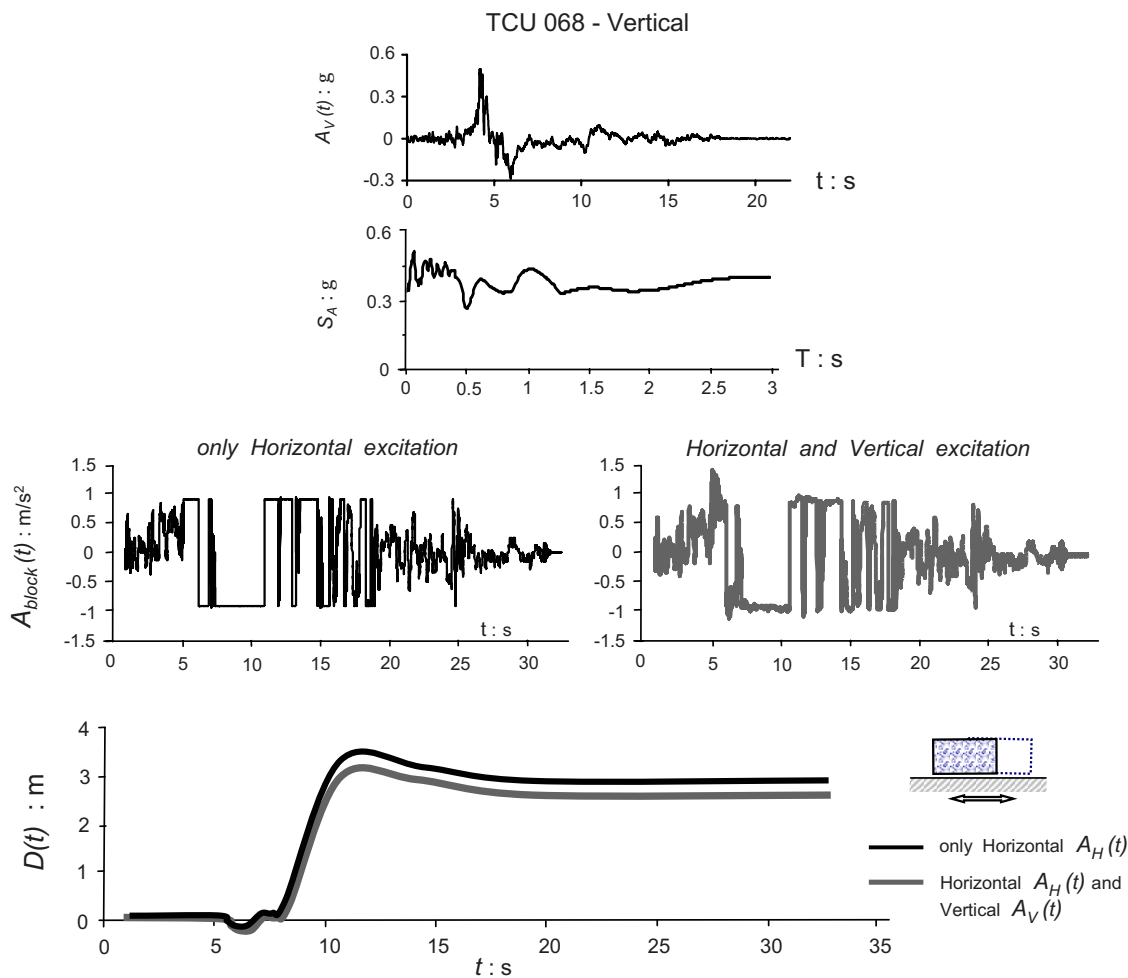


Fig. 14. Vertical component of the Chi-Chi, 1999, TCU-068 near-fault record (time history and 5% response spectrum) and its effect on horizontal acceleration and sliding displacement of the block

evidently, $\alpha_{C1} < \alpha_{C2}$. Since the geotechnical interest is usually in relatively large values of β (e.g., $\beta > 20^\circ$) and small values of the coefficient of friction ($\mu < 0.70$), the ratio $\alpha_{C2}/\alpha_{C1} \gg 1$. Thus, there is practically only one limiting acceleration

$$\alpha_C \equiv \alpha_{C1} \quad (5)$$

and α_{C2} can be considered as infinitely large. This of course should not be unduly generalized: mild slopes and lined landfills, for example, will sustain both downward and upward asymmetric sliding. The results of such an asymmetric sliding are reported herein in Fig. 20, for an inclination $\beta=5^\circ$ of the base.

As long as the upward base acceleration $\alpha_H(t)$ does not exceed α_C the block remains attached to its base, with the acceleration $\alpha_H(t)$ of the base. Sliding downhill occurs whenever $\alpha_H(t) > \alpha_C$. Throughout sliding the acceleration remains constant equal to α_C . The movement continues until the velocities of the block and the ground equalize. Knowing the critical acceleration and the time history of base excitation, permanent displacements in every sliding period are calculated by a straightforward integration process. Thanks to the transient nature of the earthquake loading, even if the block is subjected to a number of acceleration pulses higher than its critical acceleration, it may only experience a small permanent deformation rather than complete failure.

Idealized Excitation: Dimensional Analysis

The nondimensional expressions [Eq. (2)] outlined in the previous chapter are also valid in this case with a small modification

$$\frac{DA_H}{V_H^2} = F_{\text{unc}} \left(\frac{a_C}{a_H}; \beta; \text{shape of pulse, sequence of pulse;} \right. \\ \left. \text{parallel or horizontal excitation; + or - direction} \right) \quad (6)$$

The validity of this expression is demonstrated in Fig. 15, with two excitations: a Ricker wavelet and one-cycle sine, for a broad range of frequencies. Results are presented here only for $\beta=25^\circ$ which essentially ensures exclusively downward slippage.

Near-Fault Accelerograms: Some Results

A characteristic example showing the evolution of acceleration, velocity, and sliding displacement of a block the base of which is excited with the fling-affected TCU-068-NS record is illustrated in Fig. 16. The very small value of the chosen critical acceleration ratio, $\alpha_C/\alpha_H=0.05$, leads understandably to a large (maximum = residual) slippage. But notice that this is primarily the outcome

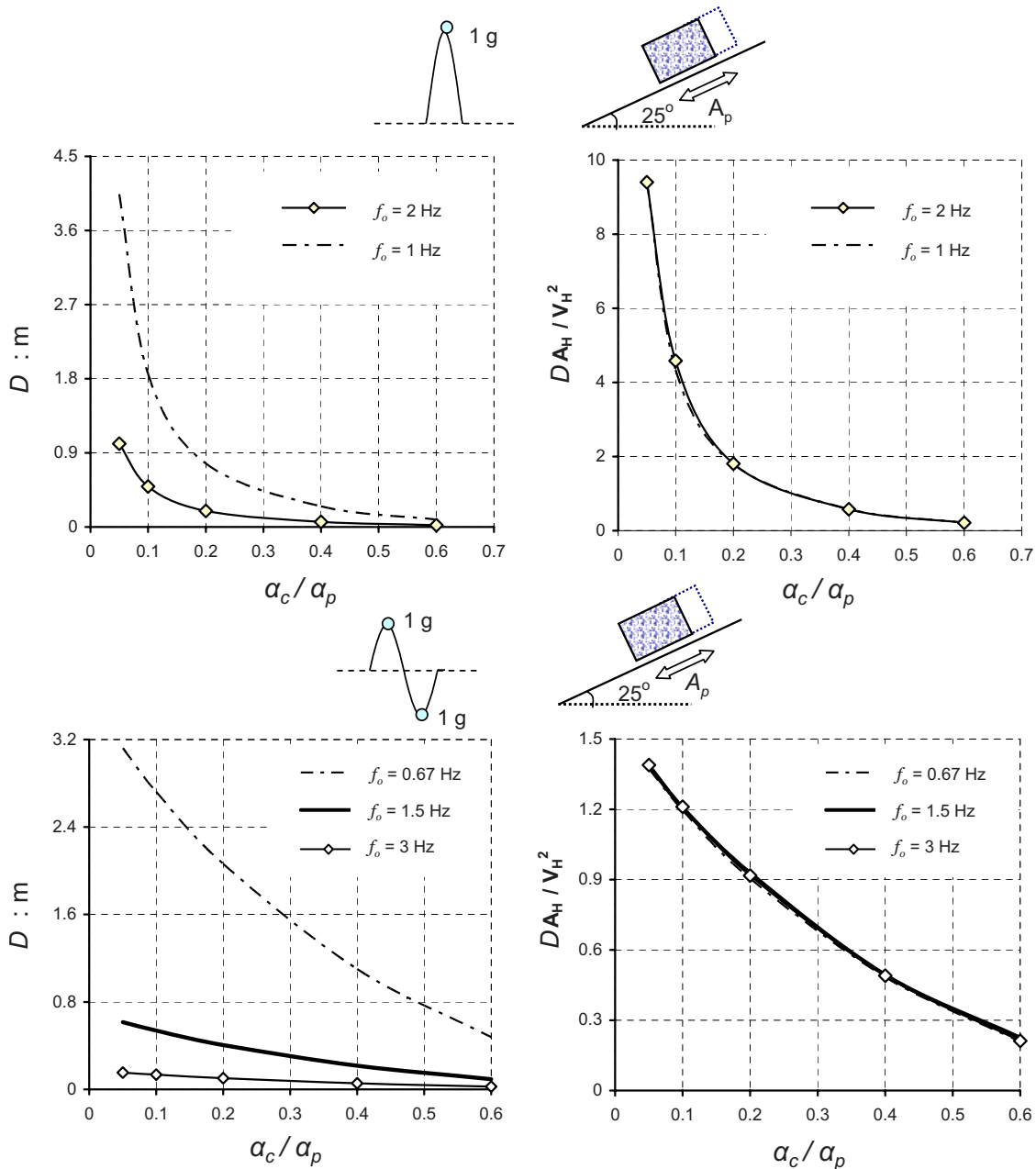


Fig. 15. Normalization effect of sliding spectra in case of a T-Ricker wavelet and a sinusoidal wavelet of one cycle. Observe that dimensional slippage curves (left figures) vary with frequency f_o whereas the normalized slippage curves (right plots) converge to a single line.

of the sequence of the few long-duration pulses between about 3.3 and 8.9 s. It is precisely those pulses that constitute the substantial fling of this record.

In this asymmetric-sliding case, the direction (+ or -) of the base excitation can be of great significance. This is because the direction determines if the most “deleterious” pulses of the record tend to move the block uphill or downhill. Thus, Fig. 17 portrays for two excitation directions (+ and -) the response of a sliding block with $\alpha_c/\alpha_H=0.1$ subjected to the directivity-affected Rinaldi record.

It is evident that completely different velocity and sliding histories are experienced by the same block to the same excitation depending on the orientation of the inclined plane. The explanation is straightforward: the highest-amplitude pulse, $A_H \approx 0.90g$

$t \approx 3.6$ s, in one case provides the driving downward inertia “force” (right-hand side plot), while in the opposite case it provides the “braking” upward inertia (left-hand side plot).

Fig. 18 completes the preceding comparison for three different critical acceleration ratios: $\alpha_c/\alpha_H=0.05, 0.10,$ and 0.2 . Apparently, for this particular excitation the direction-related difference increases. Although not shown here, when the TCU-068 record of Fig. 12 were inverted, a slippage of 25 m rather than 8 m occurred! The importance of these findings can hardly be overstated: two identical neighboring slopes, one opposite to the other (i.e., as in a canal), or the two slopes of a tall embankment, may experience vastly different sliding deformations during near-fault shaking!

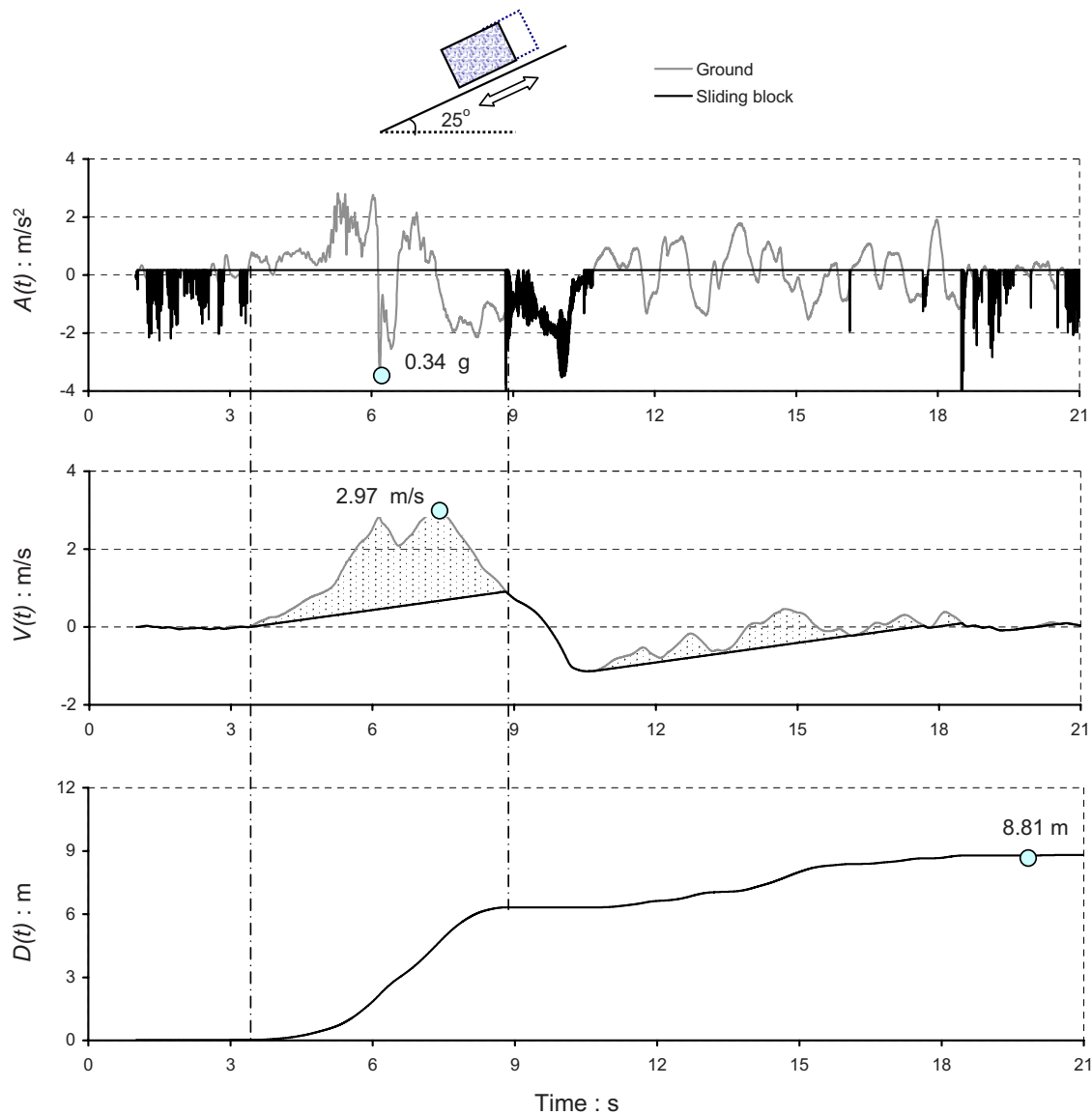


Fig. 16. Asymmetric response time histories for the TCU-068 NS ground motion ($\beta=25^\circ$ and $\alpha_C/\alpha_P=0.05$). The 8.8 m of total slippage is induced by a large sequence of remarkably long duration acceleration pulses. Observe the outstanding ground velocity pulse of almost 6 s duration and 3 m/s amplitude.

Nonparallel and Vertical Excitation

The significance of the more realistic assumption of applying the base motion *horizontally* rather than parallel to the slope, and at the same time imposing the vertical acceleration time history, are highlighted in Figs. 19 and 20. In this case the downward-sliding acceleration, α_C , is time dependent, since it is affected by the normal to the slope component of motion.

From Fig. 19 we conclude that for the TCU-068 record the horizontal excitation leads to increased (by about 20%) slippage, but the simultaneous application of the vertical component of this record has a negligible effect (which actually is beneficial in this particular case). In Fig. 20 the preceding results are recast in the form of

$$D = F(\alpha_C/\alpha_H; \beta = 5^\circ \text{ and } 25^\circ; \text{TCU-068}) \quad (7)$$

and then compared with those corresponding to the Rinaldi record (horizontal and vertical components). Evidently, the aforesaid conclusion is fully verified: in both cases, despite the record-high vertical accelerations, far exceeding the typical values, the slippage of the block is practically unaffected by the vertical component.

Epitome: Comparison

Although it was not a main goal of this paper to provide design curves for sliding displacements, it is worth comparing the results of our study against the classical relevant charts for sliding published by Makdisi and Seed (1978) and Ambraseys and Sarma (1967). The comparison is portrayed in Fig. 21. Evidently, for small α_C/α_H values (<0.30), these classical curves, based on

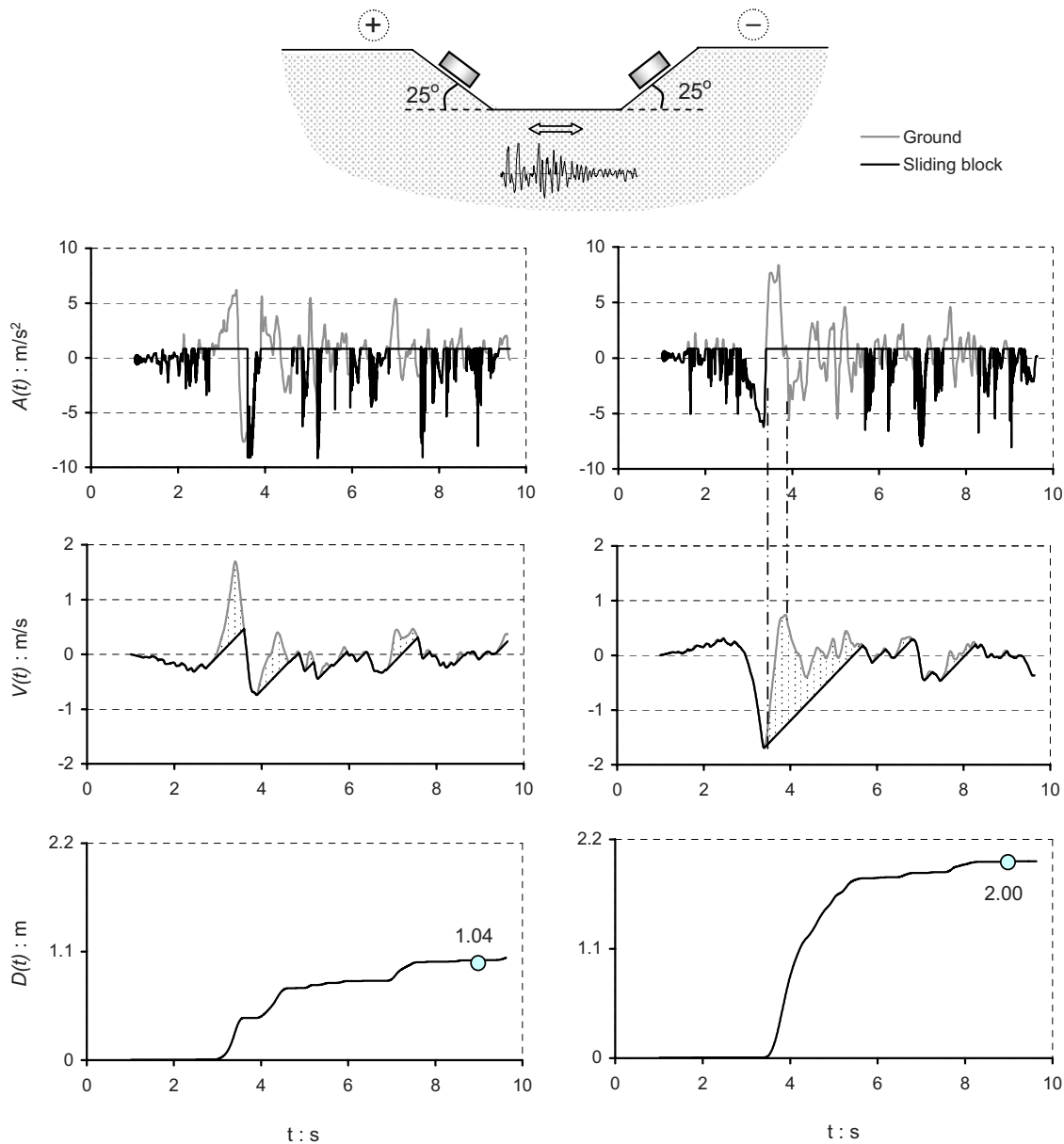


Fig. 17. Acceleration, velocity, and displacement time histories for the Rinaldi record (228° component) when imposed parallel to the sliding interface (inclination angle $\beta=25^\circ$ and $\alpha_C/\alpha_P=0.1$). Notice the asymmetric response of the block when the excitation is inverted (plots in right); the well-shaped forward-directivity pulse, shown between the dotted lines, now causes a major slippage of 2 m.

statistically processing a huge number of (mostly “usual”) records, cannot adequately predict the extreme slippage produced with motions strongly affected by fling and directivity phenomena. Our data, admittedly not of a sufficient number to allow derivation of a reliable design diagram, *do* nevertheless point out that the upper bound of sliding displacements may be substantially higher than is usually considered on the basis of widely used, if older, charts.

Conclusions

Whether on a horizontal or on an inclined base, the slippage of a rigid block subjected to near-fault directivity or fling affected

motions is sensitive not only to the peak acceleration, peak velocity, or dominant frequency, of the main excitation pulse(s) that such motions contain, but also:

- On the unpredictable detailed sequence of strong pulses.
- On the direction (+ or -) in which the shaking of an inclined plane is imposed.

Such a sensitivity of sliding to the details of the excitation has also been pointed out by previous researchers (e.g., Franklin and Chang 1977; Yegian et al. 1991a; Kramer and Lindwall 2004; Bray and Travararou 2007) who compiled the results of huge number of analyses and performed statistical analyses to derive *design sliding curves*.

By contrast, the slippage is not affected to any measurable

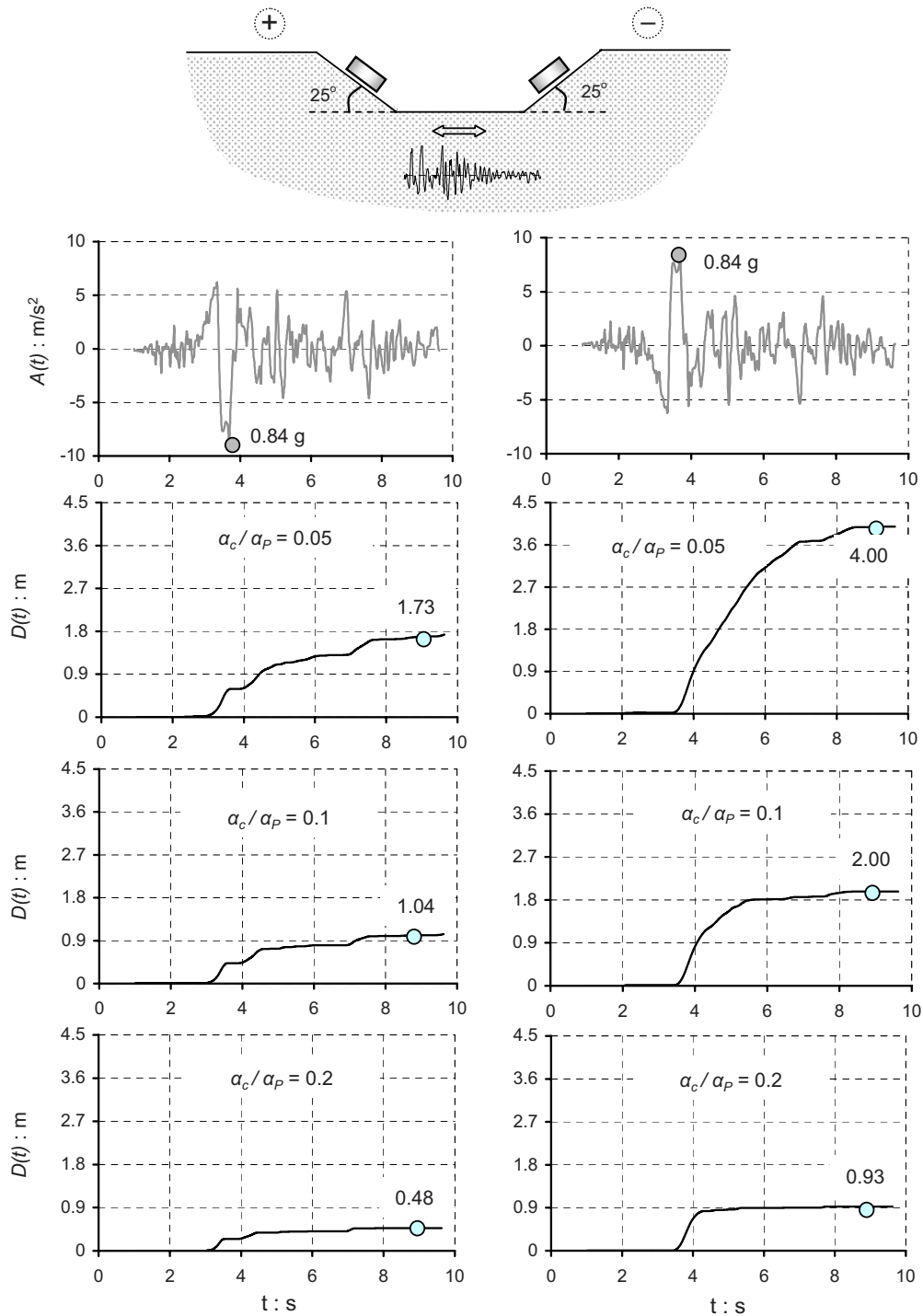


Fig. 18. Effect of excitation polarity on asymmetric sliding for the Rinaldi record (228° component, inclination angle $\beta=25^\circ$)

degree by even the strongest vertical components of accelerograms! Several paradoxical results have been illustrated and, we hope, convincingly explained in the paper. Among other findings, it was shown that in many cases, slippage only poorly correlates with the Arias intensity of the base excitation. Valuable insight has been gained into the nature of sliding and the role of near-fault motions. To answer the question posed by Abrahamson (2001): fling and directivity do matter, a lot.

Notation

The following symbols are used in this paper:

- A_C = critical yielding acceleration of the block = α_{CG} ;
- A_H = peak horizontal ground acceleration = α_{HG} ;
- A_P = peak ground acceleration applied parallel to the slope = α_{PG} ;
- A_V = peak vertical ground acceleration = α_{VG} ;

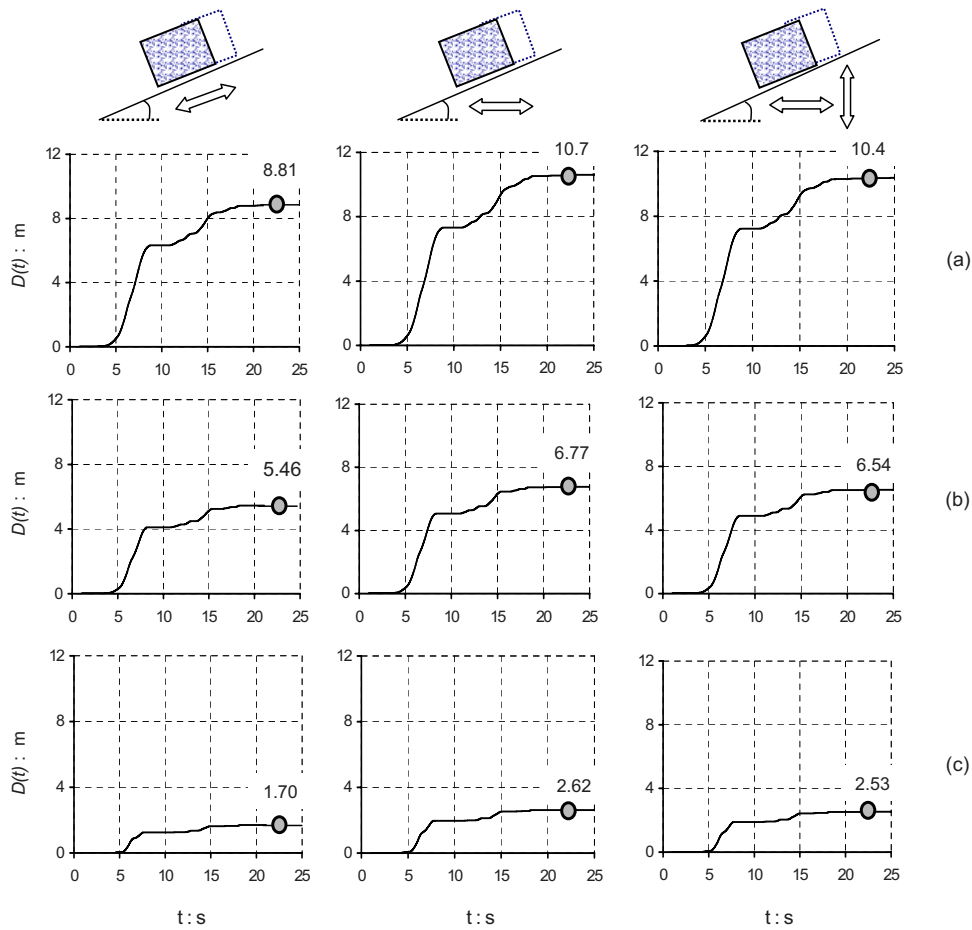


Fig. 19. Effect of horizontal and vertical acceleration on slippage for the TCU-068 record, inclination angle $\beta=25^\circ$, and acceleration ratio: (a) top line figures— $\alpha_C/\alpha_H=0.05$; (b) middle line plots— $\alpha_C/\alpha_H=0.1$; and (c) bottom line figures— $\alpha_C/\alpha_H=0.2$. The simultaneous presence of *vertical* and *horizontal* record results in smaller or equal displacements compared to those induced by exclusively horizontal motion. However, the slippage for horizontally imposed excitation is about 30% larger than the displacement triggered from the parallel to slope ground motion.

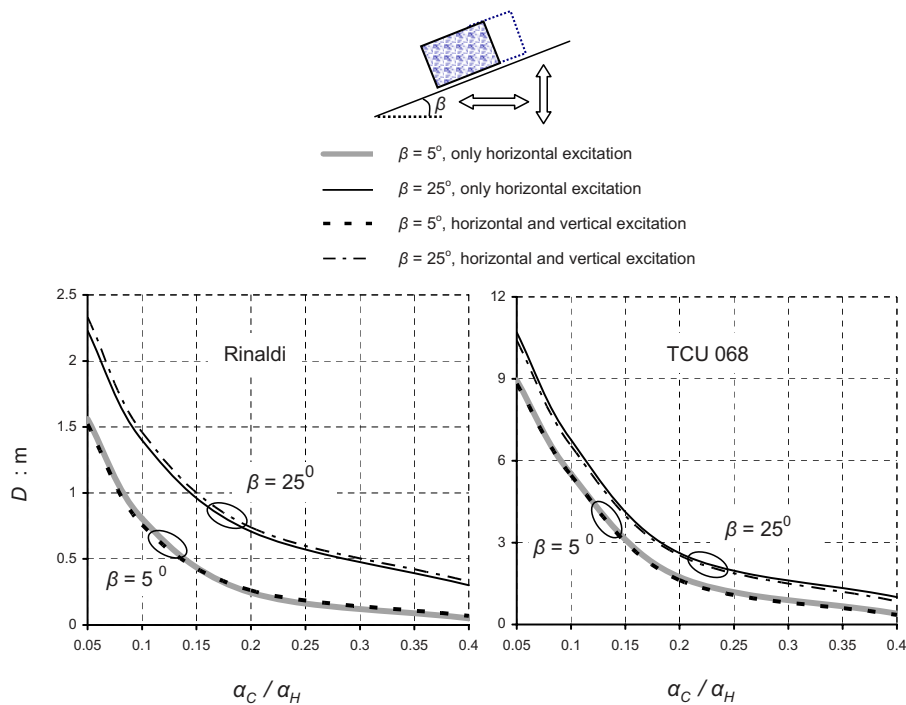


Fig. 20. Asymmetric sliding spectra illustrating the negligible effect of simultaneous vertical acceleration on the slippage produced by horizontal excitation

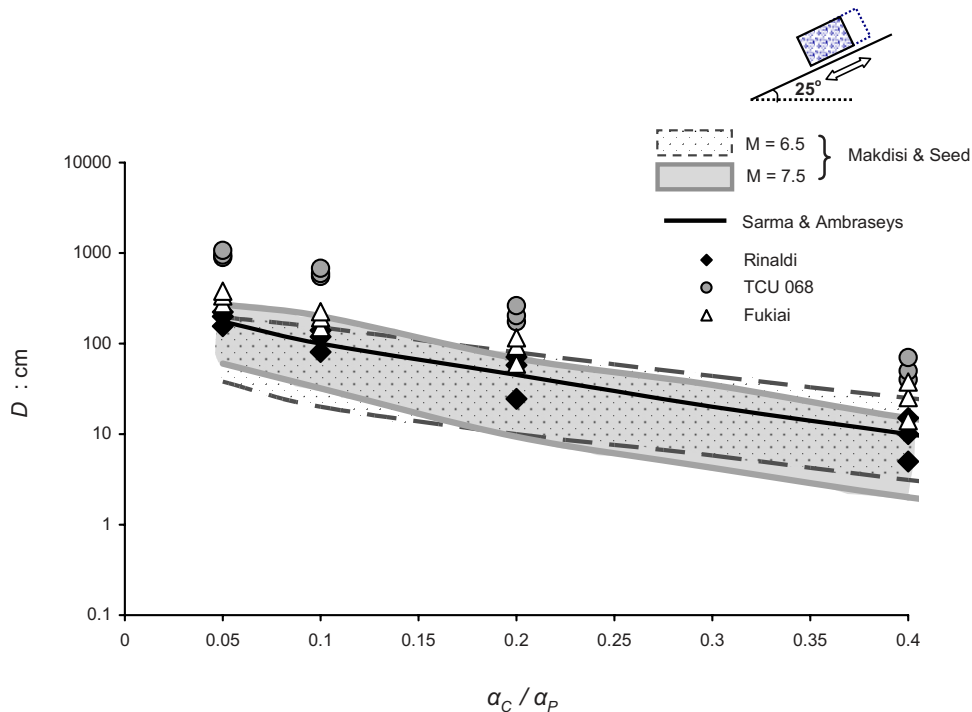


Fig. 21. Summary of our analyses: comparison with the widely used curves of Makdisi and Seed (1978) and Ambraseys and Sarma (1967) of the sliding response induced by the components of the TCU-068, Fukiai, and Rinaldi records. Each excitation is imposed in both the + and – direction.

- D = maximum sliding displacement;
 D_{res} = residual (permanent) sliding displacement;
 f_0 = dominant frequency of ground excitation;
 M = earthquake magnitude;
 T_V = dominant period of vertical motion;
 t = time;
 V_H = peak horizontal ground velocity;
 $\alpha_C = A_C/g$; $\alpha_H = A_H/g$, $\alpha_V = A_V/g$;
 α_{C1} = critical upward sliding acceleration of the block (in terms of g s);
 α_{C2} = critical downward sliding acceleration of the block (in terms of g s);
 β = angle of the inclined plane measured from the horizontal plane;
 ΔV = maximum velocity step (a la Bertero et al. 1976); and
 μ = Coulomb's coefficient of friction.

References

- Abrahamson, N. A. (2001). "Incorporating effects of near fault tectonic deformation into design ground motions." *University at Buffalo MCEER: Friedman F. V. professional program, webcast*.
 Alavi, B., and Krawinkler, H. (2000). "Consideration of near-fault ground motion effects in seismic design." *Proc., 12th World Conf. on Earthquake Engineering*, New Zealand Society for Earthquake Engineering, Auckland, New Zealand.
 Ambraseys, N. N., and Sarma, S. K. (1967). "The response of earth dams to strong earthquakes." *Geotechnique*, 17, 181–213.
 Ambraseys, N. N., and Srbulov, M. (1995). "Earthquake induced displacements of slopes." *Soil Dyn. Earthquake Eng.*, 14(1), 59–72.
 Bertero, V. V., et al. (1976). "Establishment of design earthquakes: Evaluation of present methods." *Proc., Int. Symp. on Earthquake Structural Engineering*, Vol. 1, Univ. of Missouri-Rolla, Rolla, Mo., 551–580.
 Bertero, V. V., Mahin, S. A., and Herrera, R. A. (1978). "Aseismic design implications of near-fault San Fernando earthquake records." *Earthquake Eng. Struct. Dyn.*, 6, 31–42.
 Bray, J. D., and Rathje, E. M. (1998). "Earthquake-induced displacements of solid-waste landfills." *J. Geotech. Geoenviron. Eng.*, 124(3), 242–253.
 Bray, J. D., and Rodriguez-Marek, A. (2004). "Characterization of forward-directivity ground motions in the near-fault region." *Soil Dyn. Earthquake Eng.*, 24, 815–828.
 Bray, J. D., and Travararou, T. (2007). "Simplified procedure for estimating earthquake-induced deviatoric slope displacements." *J. Geotech. Geoenviron. Eng.*, 133(4), 381–392.
 Changhai, Z., Shuang, L., Xie, L. L., and Yamin, S. (2007). "Study on inelastic displacement ratio spectra for near-fault pulse-type ground motions." *Earthquake Eng. Struct. Dyn.*, 6(4), 351–356.
 Constantinou, M. C., and Gazetas, G. (1987). "Probabilistic seismic sliding deformations of earth dams and slopes." *Proc., Specialty Conf. on Probabilistic Mechanics and Structural Reliability*, ASCE, New York, 318–321.
 Constantinou, M. C., Gazetas, G., and Tadjbakhsh, I. (1984). "Stochastic seismic sliding of rigid mass against asymmetric coulomb friction." *Earthquake Eng. Struct. Dyn.*, 12, 777–793.
 Danay, A., and Adeghe, L. N. (1993). "Seismic induced slip of concrete gravity dams." *J. Struct. Eng.*, 119(1), 108–1129.
 Fardis, N., Georgarakos, P., Gazetas, G., and Anastasopoulos, I. (2003). "Sliding isolation of structures: Effect of horizontal and vertical acceleration." *Proc., FIB Int. Symp. on Concrete Structures in Seismic Regions* (CD-ROM), Federation Internationale du Beton, Federal Institute of Technology, Lausanne, Switzerland.
 Fennes, G., and Chopra, A. K. (1986). "Simplified analysis for earthquake resistant design of concrete gravity dams." *Rep. No. UBC/EERC-85/10*, Univ. of California, Berkeley, Calif.
 Fishman, K. L., Mander, J. B., and Richards, R. (1995). "Laboratory study of seismic free-field response of sand." *Soil Dyn. Earthquake Eng.*, 14, 33–43.

- Franklin, A., and Chang, F. K. (1977). "Earthquake resistance of earth and rock-fill dams." *Rep. No. 5*, Soils and Pavements Laboratory, U.S. Army Engineer Waterways Experiment Station, Vicksburg, Miss.
- Garini, E., and Gazetas, G. (2007). "Sliding of rigid block on sloping plane: The surprising role of the sequence of long-duration pulses." *Proc., 2nd Japan-Greece Workshop on Seismic Design, Observation, and Retrofit of Foundations*, Japan Society of Civil Engineers, Tokyo, 79–104.
- Gazetas, G. (1996). *Soil dynamics and earthquake engineering: Case histories*, Chap. 5, Symeon, Athens, Greece, 269–317.
- Gazetas, G., Debchaudhury, A., and Gasparini, D. A. (1981). "Random vibration analysis for the seismic response of earth dams." *Geotechnique*, 31(2), 261–277.
- Gazetas, G., and Uddin, N. (1994). "Permanent deformation on pre-existing sliding surfaces in dams." *J. Geotech. Eng.*, 120(11), 2041–2061.
- Hall, J. F., Heaton, T. H., Halling, M. W., and Wald, D. J. (1995). "Near-source ground motion and its effects on flexible buildings." *Earthquake Spectra*, 11(4), 569–605.
- Haward, J. K., Tracy, C. A., and Burns, R. G. (2005). "Comparing observed and predicted directivity in near-source ground motion." *Earthquake Spectra*, 21(4), 1063–1092.
- Hisada, Y., and Bielak, J. (2003). "A theoretical method for computing near-fault ground motions in layered half-spaces considering static offset due to surface faulting, with a physical interpretation of fling step and rupture directivity." *Bull. Seismol. Soc. Am.*, 93(3), 1154–1168.
- Iwan, W. D., Huang, C.-T., and Guyader, A. C. (2000). "Important features of the response of inelastic structures to near-fault ground motion." *Proc., 12th World Conf. on Earthquake Engineering*, Paper No. 1740, New Zealand Society for Earthquake Engineering, Auckland, New Zealand.
- Jangid, R. S., and Kelly, J. M. (2001). "Base isolation for near-fault motions." *Earthquake Eng. Struct. Dyn.*, 30, 691–707.
- Kramer, S. L. (1996). *Geotechnical earthquake engineering*, Prentice-Hall, Upper Saddle River, N.J.
- Kramer, S. L., and Lindwall, N. W. (2004). "Dimensionality and directionality effects of Newmark stability analysis." *J. Geotech. Geoenviron. Eng.*, 130(3), 303–315.
- Kramer, S. L., and Smith, M. (1997). "Modified Newmark model for seismic displacements of compliant slopes." *J. Geotech. Geoenviron. Eng.*, 123(7), 635–644.
- Leger, P., and Katsouli, M. (1989). "Seismic stability of concrete gravity dams." *Earthquake Eng. Struct. Dyn.*, 18, 889–902.
- Lin, J. S., and Whitman, R. V. (1983). "Decoupling approximation to the evaluation of earthquake-induced plastic slip in earth dams." *Earthquake Eng. Struct. Dyn.*, 11, 667–678.
- Makdisi, F. I., and Seed, H. B. (1978). "Simplified procedure for estimating dam and embankment earthquake induced deformations." *J. Geotech. Engrg. Div.*, 104(7), 849–867.
- Makris, N., and Roussos, Y. S. (2000). "Rocking response of rigid blocks under near-source ground motions." *Geotechnique*, 50(3), 243–262.
- Mavroeidis, P. G., Dong, G., and Papageorgiou, S. A. (2004). "Near-fault ground motions, and the response of elastic and inelastic single-degree-of-freedom (SDOF) systems." *Earthquake Eng. Struct. Dyn.*, 33, 1023–1049.
- Mavroeidis, P. G., and Papageorgiou, S. A. (2003). "A mathematical representation of near-fault ground motions." *Bull. Seismol. Soc. Am.*, 93(3), 1099–1131.
- Newmark, N. M. (1965). "Effects of earthquakes on dams and embankments." *Geotechnique*, 15(2), 139–160.
- Pavlou, E. A., and Constantinou, M. C. (2004). "Response of elastic and inelastic structures with damping systems to near-field and soft-soil ground motions." *Eng. Struct.*, 26, 1217–1230.
- Rathje, E. M., and Bray, J. D. (2000). "Nonlinear coupled seismic sliding analysis of earth structures." *J. Geotech. Geoenviron. Eng.*, 126(11), 1002–1014.
- Richards, R., and Elms, D. G. (1979). "Seismic behaviour of gravity retaining walls." *J. Geotech. Engrg. Div.*, 105(4), 449–464.
- Sarma, S. K. (1975). "Seismic stability of earth dams and embankments." *Geotechnique*, 25(4), 743–761.
- Sasani, M., and Bertero, V. V. (2000). "Importance of severe pulse-type ground motions in performance-based engineering: Historical and critical review." *Proc., 12th World Conf. on Earthquake Engineering*, Paper No. 1302, New Zealand Society for Earthquake Engineering, Auckland, New Zealand.
- Seed, H. B., and Martin, G. R. (1966). "The seismic coefficient in earth dam design." *J. Soil Mech. and Found. Div.*, 92, 25–58.
- Shen, J., Tsai, M. H., Chang, K. C., and Lee, G. C. (2004). "Performance of a seismically isolated bridge under near-fault earthquake ground motions." *J. Struct. Eng.*, 130(6), 861–868.
- Singh, J. P. (1985). "Earthquake ground motions: Implications for designing structures and reconciling structural damage." *Earthquake Spectra*, 1, 239–270.
- Somerville, P. (2000). "Seismic hazard evaluation." *Proc., 12th World Conf. on Earthquake Engineering*, Paper No. 2833, New Zealand Society for Earthquake Engineering, Auckland, New Zealand, 325–346.
- Somerville, P. (2003). "Characterization of near fault ground motions for design." *Proc., ACI Specialty Conf.*, Univ. of California, San Diego.
- Somerville, P. G., Smith, N. F., Graves, R. W., and Abrahamson, N. A. (1997). "Modification of empirical strong ground motion attenuation relations to include the amplitude and duration effects of rupture directivity." *Seismol. Res. Lett.*, 68, 199–222.
- Travasarou, T. (2003). "Optimal ground motion intensity measures for probabilistic assessment of seismic slope displacements." Ph.D. dissertation, Civil and Environmental Engineering, Univ. of California, Berkeley, Calif.
- Wartman, J., Bray, J. D., and Seed, R. B. (2003). "Inclined plane studies of the Newmark sliding block procedure." *J. Geotech. Geoenviron. Eng.*, 129(8), 673–684.
- Xie, L. L., Xu, L. J., and Rondriguez-Marek, A. (2005). "Representation of near-fault pulse-type ground motions." *Earthquake Eng. Eng. Vib.*, 4(2), 191–199.
- Xu, L. J., Rondriguez-Marek, A., and Xie, L. L. (2006). "Design spectra including effect of rupture directivity in near-fault region." *Earthquake Eng. Eng. Vib.*, 5(2), 159–170.
- Yegian, M. K., Harb, J. N., and Kadakal, U. (1998). "Dynamic response analysis procedure for landfills and geosynthetic liners." *J. Geotech. Geoenviron. Eng.*, 124(10), 1027–1033.
- Yegian, M. K., and Lahlaf, A. M. (1992). "Dynamic interface shear strength properties of geomembranes and geotextiles." *J. Geotech. Engrg.*, 118(5), 760–761.
- Yegian, M. K., Marciano, E. A., and Ghahraman, V. G. (1991a). "Earthquake induced permanent deformations: A probabilistic approach." *J. Geotech. Engrg.*, 117(1), 35–50.
- Yegian, M. K., Marciano, E. A., and Ghahraman, V. G. (1991b). "Seismic risk analysis for earth dams." *J. Geotech. Engrg.*, 117, 18–34.